

# Validation of a New Model for the Estimation of Residual Tropospheric Delay Error Under Extreme Weather Conditions

Ildikó Juni<sup>1\*</sup>, Szabolcs Rózsa<sup>1</sup>

<sup>1</sup> Department of Geodesy and Surveying, Faculty of Civil Engineering,  
Budapest University of Technology and Economics, H-1111 Budapest, Műegyetem rkp. 3., Hungary

\* Corresponding author, e-mail: [juni.ildiko@epito.bme.hu](mailto:juni.ildiko@epito.bme.hu)

Received: 26 May 2018, Accepted: 08 November 2018, Published online: 04 December 2018

## Abstract

The electromagnetic signals of the Global Navigation Satellite Systems (GNSS) satellites suffer delays while propagating through the troposphere. The tropospheric delay is a significant systematic error of GNSS positioning. For safety-of-life applications of positioning many systematic error effects are either mitigated or eliminated in the positioning solution. Space based augmentation systems provide corrections for the orbital and satellite clock error, the ionospheric effects, etc. Moreover advanced GNSS provide dual frequency code observations for civilian users to eliminate the ionospheric delays caused by the electron content of the upper atmosphere. Nevertheless tropospheric delays are still taken into account using empirical models.

For safety-of-life applications besides the accuracy of the positioning, the integrity of the positioning service is an important factor, too. The integrity information includes the maximal positioning error at an extremely rare probability level, called protection level to ensure highly reliable position solution in the aviation. The Radio Technical Commission for Aeronautics Minimum Operational Performance Standard (RTCA MOPS) recommends 0.12 m as the maximum zenith tropospheric error in terms of standard deviation. Previous studies show that this recommendation seems to be too conservative leading to a lower service availability. Therefore a more realistic integrity model has to be derived for the estimation of maximal residual tropospheric delay error.

In the recent years many advanced empirical tropospheric delay models have been formulated compared to the one recommended by the RTCA. Recently new integrity models have been derived for estimating the maximum residual tropospheric delay error using numerical weather models under real extreme weather.

The aim of this paper is to study the reliability of these models conditions. In order to achieve this, high-resolution numerical weather models were ray-traced using an improved ray-tracing algorithm to evaluate the slant and zenith tropospheric delays with the geographical resolution of  $0.1^\circ \times 0.1^\circ$ .

## Keywords

troposphere model, ray tracing, integrity model, numerical weather model

## 1 Introduction

The troposphere and the electrically neutral zone above it cause electromagnetic signal delays in GNSS measurements independent of the carrier frequency. The mean tropospheric delay is approx. 2.3 meters in the zenith direction. 90% of the delay is caused by the atmospheric gases in hydrostatic equilibrium while 10% of the delay is caused by the atmospheric water vapour.

To process the GNSS pseudorange observations properly, the tropospheric delays have to be either known or must be estimated together with the coordinate solutions. In both cases a highly accurate and reliable empirical tropospheric delay model has to be used for the calculations.

For safety-of-life applications (aviation, autonomous driving and transportation, search-and-rescue, etc.) the users need to be aware of not only the accuracy, but also the integrity of the positioning solution. The bounding box of the maximum positioning error (e.g. the protection level) must be known at the extremely rare probability level of  $10^{-7}$  to ensure that the GNSS system provides reliable positioning to the user. Although the maximum zenith tropospheric error in terms of standard deviation is recommended to be 0.12 m by the Radio Technical Commission for Aeronautics Minimum Operational Performance Standard (RTCA MOPS) [1] recent studies prove that this

value is overly conservative in certain geographical locations and seasons. [2], [3], [4].

One of the drawbacks of the RTCA recommendation of maximal tropospheric delay error is that it neglects both the geographical and seasonal variations in the performance of tropospheric delay models. Recently, an advanced residual tropospheric delay error model (ARTE) has been developed that accounts for both the geographical and seasonal variations [5]. However, [5] introduces the preliminary results of tropospheric residual error model development and it does not cover the validation of the model.

The current paper studies the validation of the residual tropospheric error model proposed in [3] using high-resolution numerical weather prediction models in Central-Europe applying a modified ray-tracing approach. A similar approach is used in [6] to derive reference tropospheric delays for a benchmark dataset for the evaluation of GNSS processing techniques. However, the applied mathematical algorithm is not presented in [6].

To validate the ARTE model, an extremely rainy period was chosen at Zadar, Croatia, when a heavy precipitation of 100–200 mm in a few hours was experienced. The numerical weather models have been used to model the real atmospheric conditions during this period. The Aire Limitée Adaptation Dynamique Développement International - Limited Area Dynamic Adaptation International Development (ALADIN) [7] meteorological parameters with the horizontal resolution of  $0.1^\circ \times 0.1^\circ$  was used including all the available 32 pressure levels between 1000 hPa and 10 hPa. Since the currently widely used 2D raytracing algorithm was developed for low resolution global numerical weather models [8], where the signal path remains within the vertical atmospheric column above the station, the algorithm needed to be further modified to consider the propagation of the satellite signals to the adjacent columns, too. Section 4.2 explains the modified algorithm in details.

The extreme precipitation enables us to study the magnitude of the residual error provided by various advanced tropospheric delay models, such as the RTCA MOPS [1] and the Askne-Nordius [9] tropospheric delay model using Global Pressure and Temperature Model 2 Wet (GPT2W) [10] meteorological parameters. Section 2 introduces these models in details. They have already been studied under nominal conditions in [11] using radiosonde observations and it was shown that the GPT2W model performs better than the original RTCA MOPS model. However radiosonde observations are available at a few stations in Central-Europe and their temporal resolution is weak, too.

Thus they are not suitable for assessing the residual tropospheric delay models for large regions with high spatial and temporal resolution.

It must also be mentioned that [12] shows an alternate approach to minimize the non-nominal tropospheric delays in satellite navigation by selecting only a subset of the available satellites in the positioning solution. However the application of this model is not compatible with the currently adopted standards of RTCA.

## 2 The studied tropospheric delay models

The total tropospheric delay is usually calculated in zenith direction (ZTD) and it can be divided into two parts, the zenith hydrostatic (ZHD) and the zenith wet (ZWD) delay [13]. The various empirical troposphere models use slightly different types of meteorological parameters as input data, such as the air temperature, the air pressure, the water vapour pressure, the temperature lapse rate and the water vapour lapse rate to calculate both ZHD and ZWD [14]. The delay substantially increases as the satellite is located closer to the horizon. The tropospheric delay models take this effect into consideration by introducing an elevation angle dependent mapping function. Depending on the source of the input meteorological data, all tropospheric models can be evaluated in blind and site modes. In blind mode models use their own built-in dataset or data stemming from the international reference atmosphere, while in-situ meteorological observations can improve the accuracy of the models in site mode.

### 2.1 RTCA MOPS model

According to the RTCA recommendations the *ZHD* and *ZWD* are calculated using five meteorological parameters: air temperature ( $T$  [K]), air pressure ( $p$  [hPa]), water vapour pressure ( $e$  [hPa]), temperature lapse rate ( $\alpha$  [K/m]) and water vapour lapse rate ( $\lambda$  [-]) [1]:

$$ZHD = \left(1 - \frac{\alpha \cdot H}{T}\right)^{\frac{g}{R_d \alpha}} \cdot \frac{10^{-6} \cdot k_1 \cdot R_d \cdot p}{g_m}, \quad (1)$$

$$ZWD = \left(1 - \frac{\alpha \cdot H}{T}\right)^{\frac{(\lambda+1)g}{R_d \alpha} - 1} \cdot \frac{10^{-6} \cdot k_3 \cdot R_d}{g_m \cdot (\lambda + 1) - \alpha \cdot R_d} \cdot \frac{e}{T}, \quad (2)$$

where  $k_1 = 77.604$  K/hPa and  $k_3 = 382000$  K<sup>2</sup>/hPa are the empirical refraction coefficients,  $R_d = 287.054$  J/kgK denotes the gas constant of dry air,  $g = 9.80665$  m/s<sup>2</sup> is the gravity acceleration,  $g_m = 9.784$  m/s<sup>2</sup> corresponds to the mean gravity acceleration and  $H$  [m] is the receiver's height above the mean sea level.

In blind mode the five meteorological parameters are calculated with the mean values and the annual variations which are built into the model and depend on the receiver latitude and the day-of-year. These values are derived from the UNB3 troposphere model [15]. The model distinguishes two cases at mapping function calculation: in the first one the elevation angle is not less than 4° [16] and the second case it is less than 4° but not less than 2°. The two formula can be merged:

$$m(E_i) = \left( \frac{1.001}{\sqrt{0.002001 + \sin^2(E_i)}} \right) \cdot \left( 1 + 0.015 \left( \max \left( 0, 4^\circ - E_i \right) \right)^2 \right), \quad (3)$$

where  $m(E_i)$  denotes the mapping function and  $E_i$  is the elevation angle of the  $i$ -th satellite.

### 2.2 GPT2W model

GPT2W is a global empirical model of surface meteorological parameters [10] and this is improved to model wet delay better compared to the original Global Pressure and Temperature Model (GPT2) [17]. GPT2W provides global models for the air temperature, the air pressure, the temperature lapse rate, the water vapour pressure and its decrease factor and the weighted mean temperature, which are derived from European Centre for Medium-Range Weather Forecasts (ECMWF) Era-Interim [18] reanalysis monthly mean data on 37 pressure level for the period of 2001–2010. The mean values, the annual and semi-annual variations of the meteorological parameters are in a global grid with resolution  $1^\circ \times 1^\circ$ . This model uses the Saastamoinen troposphere model [19] to estimate the zenith hydrostatic delay and the Askne-Nordius troposphere model [9] to calculate the zenith wet delay:

$$ZWD = 10^{-6} \cdot \left( k_2' + \frac{k_3}{T_m} \right) \cdot \frac{R_d}{(\lambda + 1) \cdot g_m} \cdot e_s, \quad (4)$$

where  $k_2' = 16.5221 \text{ K/hPa}$  és  $k_3 = 377600 \text{ K}^2/\text{hPa}$  are empirically determined coefficients,  $R_d = 286.9 \text{ J/kg/K}$  denotes the gas constant of dry air,  $e_s$  is the water vapour pressure at the site [hPa]  $T_m$  denotes is the weighted mean temperature of the water vapour [K]. The computation of the slant tropospheric delay is done using the Vienna Mapping Function (VMF1)[8].

### 3 Integrity analysis

In order to ensure safety-of-life users that the positioning solution provided by GNSS is reliable, the performance of the tropospheric delay models have to be evaluated from the integrity perspective. In such investigations, generally

the residual error of the positioning solution is quantified and investigated using statistical tools at very high confidence levels ( $4-6\sigma$ ). Since our paper focuses on the performance of the tropospheric delay model only, our studies on the residual tropospheric delays are discussed in the next parts of the paper. It must also be noted that the total residual error for GPS pseudo-range measurements are currently dominated by the ionospheric effects, rather than the troposphere [20]. However, the emerging new civilian signals available in modernized GNSS systems will significantly improve the mitigation of ionospheric effects, thus the tropospheric delays will become a dominant error source of pseudorange observations, especially for lower elevation angles [21]. The RTCA MOPS [1] specifies the currently adopted tropospheric delay model for safety-of-life users. It recommends a very conservative global constant for the estimation of maximal residual tropospheric delay error of 0.12 m in terms of standard deviation. The residual tropospheric delay error in the slant direction is calculated using an appropriate mapping function [16]:

$$\sigma_{i,tropo} = (\sigma_{TVE} \cdot m(E_i)), \quad (5)$$

$$m(E_i) = \frac{1.001}{\sqrt{0.002001 + \sin^2(E_i)}}, \quad (6)$$

where is  $\sigma_{TVE} = 0.12 \text{ m}$ .

The integrity of the tropospheric delay model is maintained, when the estimated maximal tropospheric residual error (the tropospheric protection level) overbounds the real tropospheric residual error at a very high confidence level. According to the International Civil Aviation Organization (ICAO) recommendations, the integrity of the positioning service must be maintained at the probability level of  $(1-10^{-7})$  over 150 seconds in case of approach operations with vertical guidance (APV-I and APV-II), the vertical guidance down to a decision height of 200 feet (LPV-200) and the Category I (CAT-I) precision approaches [22] [23]. Thus in our studies the vertical tropospheric protection level (VTPL) is calculated as:

$$VTPL = K_V \cdot \sigma_{i,tropo}, \quad (7)$$

where  $K_V = 5.33$  [1] is the value of the probability density function of the standard normal distribution at the probability level of  $10^{-7}$ .

Recently, new global models have been derived for the estimation of the maximal residual tropospheric delay error using the extreme value theory in [5]. These models

consider both the geographical and the seasonal variations of the maximal residual tropospheric delay error, and provide the empirical input parameters for 18 latitude bands of  $10^\circ$  for the whole globe for both the hydrostatic ( $\delta_{HVE}$ ) and wet ( $\delta_{WVE}$ ) tropospheric zenith delays separately.

At Zadar, Croatia (N44.1, E15.2) the hydrostatic and wet error can be calculated with the given parameters in the latitude band of  $N40^\circ$ – $50^\circ$  for any time of the year. To determine the slant errors Eqs. (5–6) are used with the hydrostatic and wet delay error.

**4 Generating the reference data using ray tracing**

The aim of this work is to evaluate and validate the various maximal tropospheric delay error models under an extreme weather scenario based on numerical weather model data. In order to calculate the residual tropospheric delay error, the tropospheric delay caused by the real atmosphere must be calculated as reference data, and the tropospheric delays estimated by the various models will be subtracted from these reference models to obtain the residual error. In this section the calculation of the reference data sets using numerical weather models is discussed.

**4.1 Input data**

ALADIN [7] is a regional numerical weather analysis and forecast model that contain different meteorological data in a grid with the resolution of  $0.1^\circ \times 0.1^\circ$ . The ALADIN model provided by the Hungarian Meteorological Service covers Europe between the latitudes of  $37^\circ$ – $56^\circ$  and the longitudes of  $2^\circ$ – $31^\circ$ . Daily 4 analysis datasets (00, 06, 12, 18 UTC) of geopotential, temperature and specific humidity values were used for the period 7.5–13.5 September 2017 on 32 pressure level (1000hPa-10hPa) for this study, where 7.5 identifies the day of the month (DOM), thus the starting time of the corresponding 6-hour-interval (7/09/2017 UTC 12–18). In order to consider the delay effects of the higher neutral atmosphere, the International Standard Atmosphere (ISA) [24] data were used to extend the vertical profiles of meteorological data up to 86000 m.

**4.2 Calculation of the reference tropospheric delays**

Slant tropospheric delays can be calculated by ray tracing the numerical weather models of the neutral atmosphere along the path of the satellite signal. The ray is started at the location of the receiver at a certain elevation angle and refracts at the boundary of each atmospheric layer. Thus the distance travelled in each atmospheric layer can be calculated as a function of the elevation angle and the width of the layer.

In order to minimize the error of the latter numerical integration, the vertical resolution of the input data was increased by interpolation. Firstly the resolution of the height is increased in a pre-defined manner given in [25]. The temperature was interpolated linearly in the vertical profiles, while the pressure and the water vapour pressure were interpolated exponentially.

It must be mentioned, that the original ray-tracing method given in [8] was developed for the ray-tracing of global numerical weather models with the resolution of a few degrees. Thus it did not consider the case when the ray leaves the vertical column of the atmospheric profile above the station and continues its path in one of the adjacent vertical columns. However, due to the high horizontal resolution ( $0.1^\circ$ – $8$  km) of the applied local numerical weather model, this case had to be considered, too.

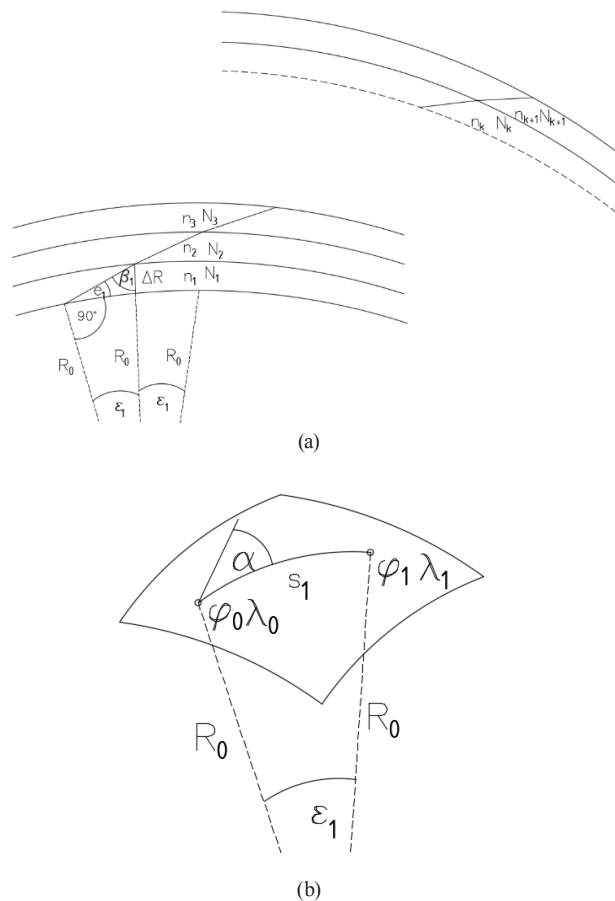


**Fig. 1** The principle of the improved ray-tracing method a) Side view with refracted ray in the atmospheric layers, where  $\beta_1$  is the incident angle,  $R_0$  is the radius of the Earth,  $\Delta R$  is the width of the layer and  $e_1$  is the elevation angle,  $\epsilon_1$  denotes the central angle,  $N$  is the refractivity and  $n$  is the refractivity index. b) The calculation of the geographical coordinates of the piercing point projected to the Earth surface, where  $\alpha$  is the azimuth,  $s_1$  is the length of the refracted

The principle of the modified approach is that not only the elevation of the piercing point of the satellite-receiver ray at the boundary of atmospheric layer is calculated, but also its geographical coordinates are computed. Since these coordinates usually do not coincide with the grid points of the numerical weather model, at each level a bilinear interpolation of the meteorological parameters is used to estimate the value of the parameter at the intersection. Thus, the improved ray-tracing method requires the determination of the coordinates where the ray reaches the boundary of the layer. Fig 1. depicts the geometry of this calculation. Firstly, the incident angle ( $\beta_1$ ) is calculated from the vertical section formed by the satellite-receiver path and the Earth's center in the lowest atmospheric layer:

$$\beta_1 = \arcsin \frac{R_0 \cdot \sin(e_1 + 90^\circ)}{\Delta R + R_0}, \quad (8)$$

where  $R_0$  is the radius of the Earth,  $\Delta R$  is the width of the layer and  $e_1$  is the elevation angle. The central angle ( $\varepsilon$ ) can be calculated using the sum of the inner angles of the triangle.

Secondly, the geographical coordinates of the piercing point are calculated using spherical approximation:

$$\varphi_1 = \arcsin(\cos \varepsilon_1 \cdot \sin \varphi_0 + \sin \varepsilon_1 \cdot \cos \varphi_0 \cdot \cos \alpha) \quad (9)$$

$$\lambda_1 = \arcsin\left(\frac{\sin \alpha \cdot \sin \varepsilon_1}{\cos \varphi_0}\right) + \lambda_0 \quad (10)$$

In order to determine the value of the meteorological parameters at the piercing point, a bilinear interpolation is done using all the four adjacent grid points.

In order to trace the ray between the receiver and the satellite, the refracted angle must be calculated using the Snell's Law. Therefore the refractivities are calculated in the adjacent atmospheric layers using the Essen-Froome equation [26]:

$$N = k_1 \cdot \frac{p_d}{T \cdot Z_d} + k_2 \cdot \frac{e}{T \cdot Z_w} + k_3 \cdot \frac{e}{T^2 \cdot Z_w}, \quad (11)$$

where  $p_d$  is the air pressure of dry air [hPa],  $Z_d$  and  $Z_w$  denote the compressibility factor of dry air and water vapor [-] and  $k_2 = 64.790$  K/hPa. Based on the refractivities, the refracted angle can be calculated using the Snell's Law. Since it is the complement angle of the elevation angle in the next atmospheric layer, an analogous calculation can be done to determine the incident and refracted angles at the next atmospheric layers. Eq. (8–10) can be. Thus, the geometry of the bent satellite-receiver ray can be reconstructed.

However, it must also be noted that the majority of the tropospheric delay stems from the propagation velocity of the signal in the atmospheric layer and the geometry has a significantly lower effect on the tropospheric delays. The total slant tropospheric delay (STD) can be estimated by the numerical solution of the Thayer-integral [27]:

$$STD = 10^{-6} \int N ds \quad (12)$$

where  $N$  is total refractivity (hydrostatic plus wet), that is integrated along the ray path between the satellite and the receiver.

For the numerical solution, the hydrostatic and wet delays caused by each atmospheric layer can be quantified as a product of the length of the ray and the hydrostatic and wet refractivity, respectively [13][26]. Finally, the total slant delays are calculated as the sum of the hydrostatic and wet delays caused by the individual atmospheric layers:

$$STD = 10^{-6} \sum_{i=1}^k N_i s_i \quad (13)$$

where  $i = 1, 2, \dots, k$ , where  $k$  is the number of the atmospheric layers,  $s_i$  denotes the length of the refracted beam,  $N_i$  is the refractivity of the given layer.

It must be noted that this improved approach provides anisotropic slant tropospheric delay estimates, since the meteorological parameters are not isotropic. Therefore the calculation should be made for different azimuths and elevation angles separately.

## 5 Results

In order to calculate the residual tropospheric delay error, firstly the hydrostatic and wet tropospheric delays are estimated using the RTCA MOPS and GPT2W tropospheric models. Afterwards, the reference delays are calculated by the improved ray tracing method.

The differences between the reference and the estimated values provide the residual tropospheric delay error. These residual error values were compared to the maximal tropospheric delay error estimated by the RTCA MOPS and the ARTE models. To carry out this validation test, a test scenario with extreme weather conditions was chosen. Between 10–11 September 2017 an extremely intense precipitation occurred in the area of Zadar, Croatia. Field observations reported that the total amount of the rainfall reached the level of 100–200 mm in a couple of hours.

For the same period, four precipitation maps per day were derived using the ALADIN model with the resolution  $0.1^\circ \times 0.1^\circ$ . The precipitation maps identified a cumulative

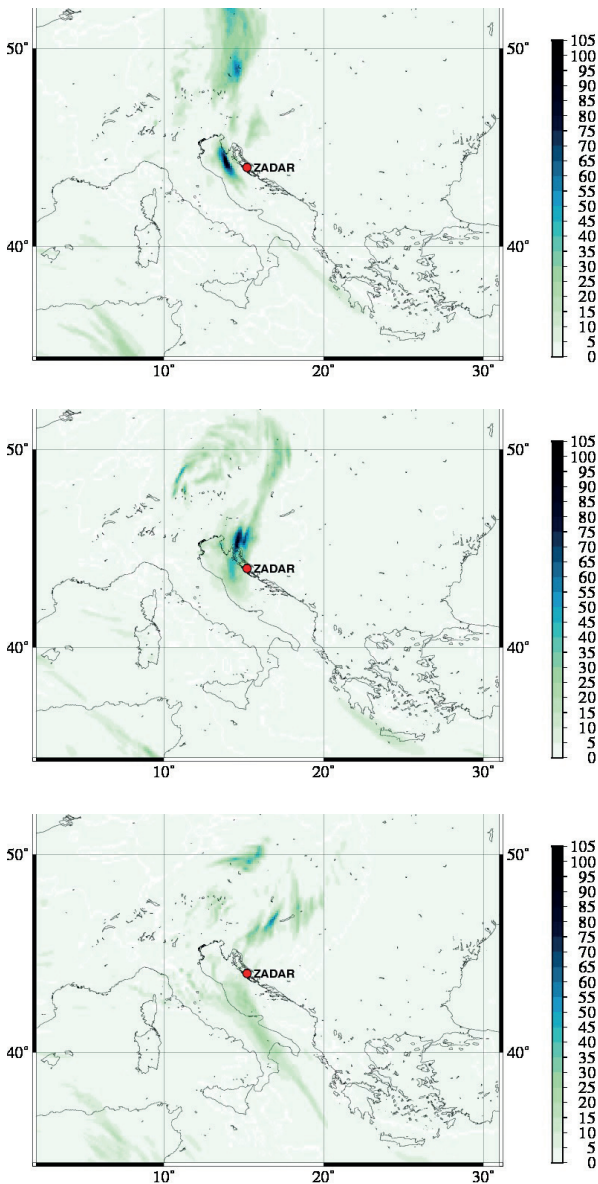


Fig. 2 Precipitation maps of 11.0, 11.25, 11.5 September 2017 at Zadar [mm]

precipitation of 59 mm at Zadar in 6 hours for 11.25 September 2017. The cumulative precipitation in 12 hours (11.25–11.5) almost reaches the level of 83 mm. These values are significantly less, than the observed ones, which can be explained by the smoothing effect of the numerical weather model. Based on the precipitation maps a rainy (11.25) and two dry periods (7.5–11.0, 11.5–13.5) are distinguished at the analysis (Fig 2).

The ARTE model gives the hydrostatic and the wet tropospheric delay error separately, while the RTCA MOPS recommendation provides a maximum residual tropospheric delay error for the total tropospheric delay. To be able to compare the performance of the two residual error models separately for the hydrostatic and the wet component, the

maximal total sigma provided by the RTCA MOPS has to be split into two separate values for the hydrostatic and wet delays. Since the ARTE model provides the ratio between the hydrostatic and wet maximum residual errors in terms of standard deviation as  $\sigma_{wv} = 1.75 \cdot \sigma_{hv}$  for the study period, the sigma of 0.12m recommended by the RTCA MOPS was separated to hydrostatic and wet sigmas keeping this ratio using the law of the propagation of uncertainties. Thus for the RTCA MOPS comparisons the following sigma values were used in the zenith direction:  $\sigma_{hv} = 0.060$  m and  $\sigma_{wv} = 0.104$  m. The residual error calculations were done using (Eq. (5–7)) in the azimuth of 135° for the elevation angles of 88° to 6° with the increments of two degrees. It must be noted that the azimuth of the satellite affects the values of the ray-traced reference data only while the estimated tropospheric delay values are isotropic. In order to assess the effect of the anisotropic reference tropospheric delays around the station, the calculations were done for several azimuths, but only marginal differences were observed in the results.

The residual tropospheric delay error values are plotted with the maximum tropospheric error of both integrity models for the whole period. Although the ARTE model takes into consideration the seasonal variation of the maximal residual tropospheric delay error, this variation during the one-week-period was less than 1%. Therefore the variation of the maximal tropospheric delay error values were neglected and the ARTE model was evaluated for the middle of the study period of 10.5 September, 2017.

The estimation of the maximum residual tropospheric delay error calculations were done using both of the RTCA MOPS and the GPT2W models in both blind and site modes for Zadar. Fig. 3. and Fig. 4 show the results obtained in blind mode and site mode, respectively. The red curve depicts the estimated maximum residual error using the ARTE model, while the orange curve shows the same error estimated using the RTCA MOPS recommendation. The calculated real tropospheric residual error values are symbolized with grey or blue crosses for the dry and the rainy period, respectively. The results have revealed that the hydrostatic delay residuals in both blind and site mode show no significant differences between the dry and wet periods. However remarkable differences can be experienced between the dry and rainy periods for the wet component in blind mode. The results agree with the expectations, which the RTCA-MOPS and the GPT2W models underestimate the wet delay in the rainy period, because of the fact that significantly higher amount of precipitation was observed in Zadar than normally in this season.

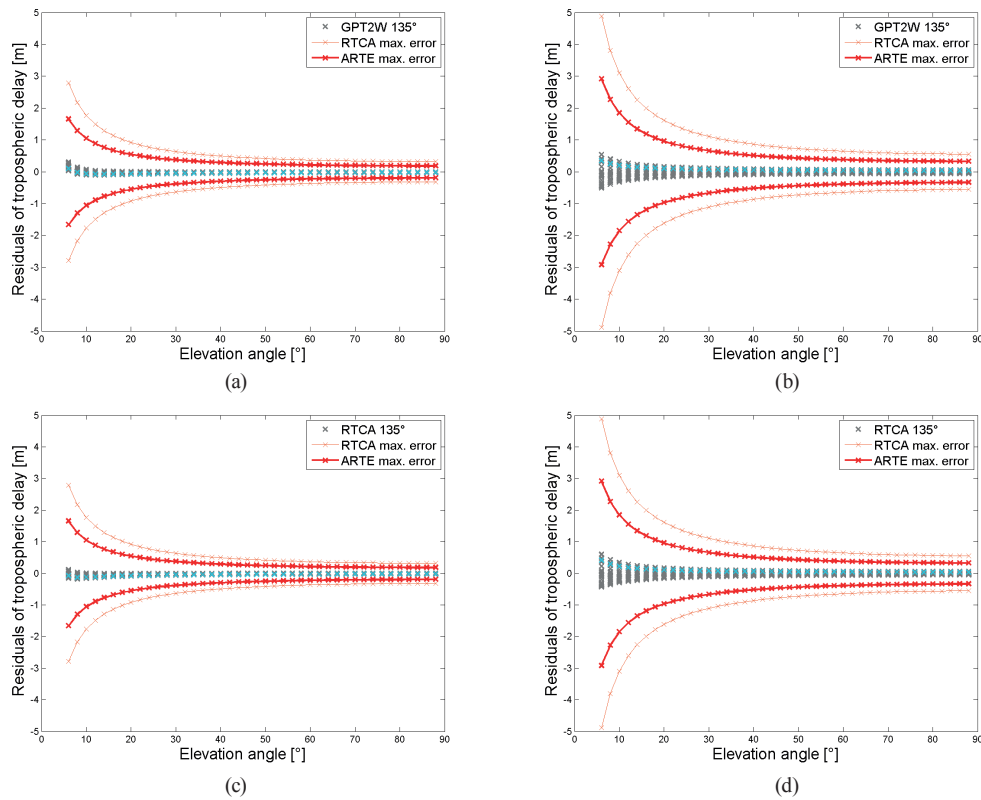


**Fig. 3** The differences between the delays of the reference and the analysed models a) GPT2W hydrostatic b) GPT2W wet c) RTCA hydrostatic and d) RTCA wet (blue: rainy) in blind mode. The maximum wet tropospheric errors of the RTCA MOPS and of the ARTE integrity model

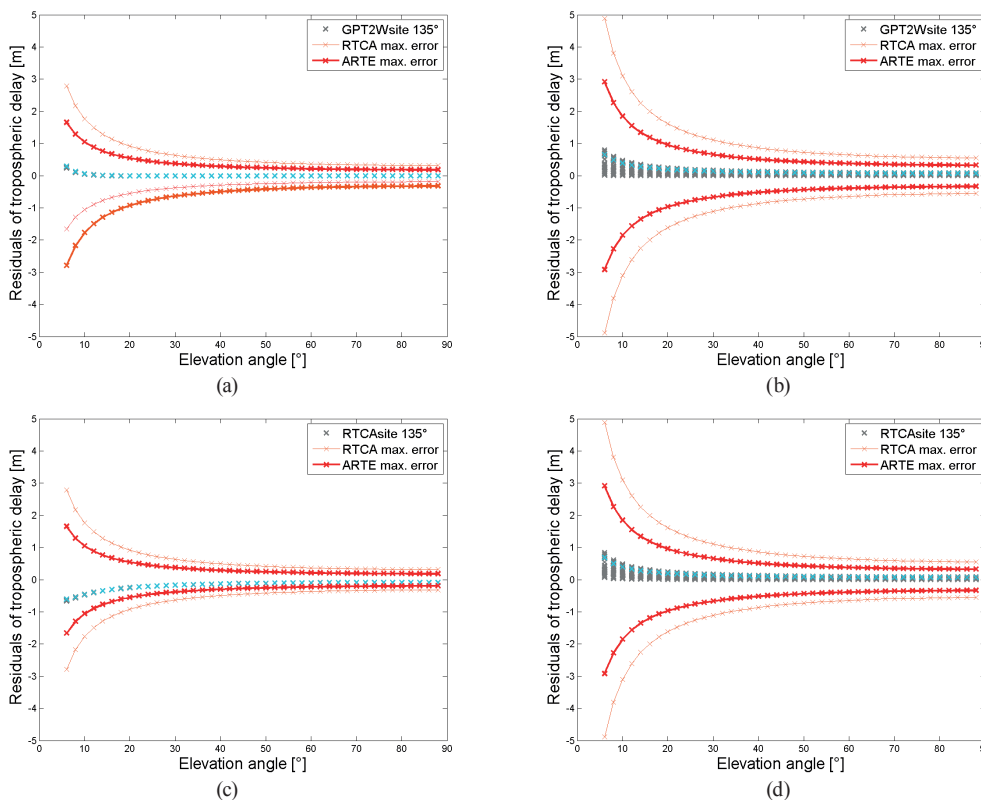


**Fig. 4** The differences between the delays of the reference and the analysed models a) GPT2W hydrostatic b) GPT2W wet c) RTCA hydrostatic and d) RTCA wet (blue: rainy) in site mode. The maximum wet tropospheric errors of the RTCA MOPS and of the ARTE integrity model

The results have also shown that both the ARTE and the RTCA MOPS models overestimate the residual tropospheric delay error for both the hydrostatic and the wet components in the study period. This confirms that both of the models can be effectively used to provide reliable maximal residual error estimates for the tropospheric delay models. The figures also clearly show that the ARTE model provides significantly lower error estimates at all the elevation angles, which proves that the ARTE model is less conservative than the RTCA MOPS model. Our case study has revealed that the ARTE model achieves the overbounding of residual tropospheric delay error with a smaller error estimate compared to the RTCA MOPS model. Thus, it could be more efficiently used for safety-of-life applications even in the studied extreme weather conditions, since it provides smaller maximal error estimates leading to a smaller protection level. This can contribute to the improvement of the availability and continuity of the satellite positioning service.

## 6 Summary and conclusions

For the safety-of-life users the coordinates obtained by the onboard GNSS receivers must be reliable. The reliability of the service can be studied using the tools of integrity analysis. Focusing on the tropospheric delays only, the current RTCA MOPS recommendations give a very conservative, global constant for the maximal residual tropospheric error of 0.12 m in terms of the standard deviation. Recently, a less conservative integrity model called ARTE was developed that takes into consideration the seasonal and geographical variations. This model was derived by the statistical analysis of residual tropospheric delay error at a high confidence levels ( $4-6\sigma$ ).

Our study focused on the validation of this models using real atmospheric conditions during an extreme weather event. In order to achieve this, an improved raytracing method was applied. The ALADIN numerical weather model data with resolution  $0.1^\circ \times 0.1^\circ$  for 7.5–13.5 September 2017, containing an extreme rainy period at Zadar (N44.1, E15.2).

Our results showed that although the ARTE model provides significantly lower maximal residual tropospheric delay error estimates, it still provides conservative estimations.

It must be noted, that small confidence interval of ARTE can improve the availability and continuity of the positioning system service. The reason of this that the accuracy expectations at a lower protection level are rarely exceeded. The ARTE model can improve these features without the development of hardware.

## Acknowledgement

Support of grant BME FIKP-VÍZ by EMMI is kindly acknowledged.

## References

- [1] RTCA "DO-253D Minimum Operational Performance Standards For GPS Local Area Augmentation System Airborne Equipment", RTCA, Inc., Washington, DC, USA, 2013.
- [2] Storm Van Leeuwen, S., Marel, H. van der, Toissaint, M., Martelucci, A. "Validation of SBAS MOPS Troposphere Model over the EGNOS Service Area", presented at Proceedings of the European Navigation Conference, Netherlands, May 16–19. 2004.
- [3] McGraw, G. A. "Tropospheric error modeling for high integrity airborne GNSS navigation", In: Proceedings of the 2012 IEEE/ION Position, Location and Navigation Symposium, Myrtle Beach, SC, USA, 2012, pp. 158–166.  
<https://doi.org/10.1109/PLANS.2012.6236877>
- [4] Leandro, R. F., Santos, M. C., Langley, R. B. "UNB Neutral Atmosphere Models: Development and Performance", In: Proceedings of the 2006 National Technical Meeting of the Institute of Navigation ION NTM, Monterey, CA, USA, 2006, pp. 564–573.
- [5] Rózsa, Sz., Ambrus, B., Juni, I. "Integrity analysis of the RTCA tropospheric delay model", In: AIS 2017 - 12th International Symposium on Applied Informatics and Related Areas, Székesfehérvár, Hungary, 2017, pp. 94–99.
- [6] Kačmařík, M., Douša, J., Dick, G., Zus, F., Brenot, H., Möller, G., Pottiaux, E., Kaplon, J., Hordyniec, P., Václavovic, P., Morel, L. "Inter-technique validation of tropospheric slant total delays", Atmospheric Measurement Techniques, 10(6), pp. 2183–2208, 2017.  
<https://doi.org/10.5194/amt-10-2183-2017>
- [7] ALADIN "The ALADIN project: Mesoscale modelling seen as a basic tool for weather forecasting and atmospheric research", WMO Bulletin, 46(4), pp. 317–324, 1997.
- [8] Boehm, J., Schuh, H. "Vienna Mapping Functions", In: Proceedings of the 16th Working Meeting on European VLBI for Geodesy and Astrometry, Leipzig, Germany, 2003, pp. 131–143.
- [9] Askne, J., Nordius, H. "Estimation of tropospheric delay for microwaves from surface weather data", Radio Science, 22(3), pp. 379–386, 1987.  
<https://doi.org/10.1029/RS022i003p00379>
- [10] Böhm, J., Möller, G., Schindelegger, M., Pain, G., Weber, R. "Development of an improved empirical model for slant delays in the troposphere (GPT2w)", GPS Solutions, 19(3), pp. 433–441, 2015.  
<https://doi.org/10.1007/s10291-014-0403-7>
- [11] Rózsa, S. "Modelling Tropospheric Delays Using the Global Surface Meteorological Parameter Model GPT2", Periodica Polytechnica Civil Engineering, 58(4), pp. 301–308, 2014.  
<https://doi.org/10.3311/PPci.7267>
- [12] Wang, Z., Xin, P., Li, R., Wang, S. "A method to reduce non-nominal troposphere error", Sensors, 17(8), p. 1751, 2017.  
<https://doi.org/10.3390/s17081751>
- [13] Smith, E. K., Weintraub, S. "The Constants in the Equation for Atmospheric Refractive Index at Radio Frequencies", Journal of Research of the Notional Bureau of Standards, 50(1), pp. 39–41, 1953.  
<https://doi.org/10.1109/JRPROC.1953.274297>

- [14] Mekik, C., Deniz, I. "Modelling and validation of the weighted mean temperature for Turkey", *Meteorological Applications*, 24(1), pp. 92–100, 2017.  
<https://doi.org/10.1002/met.1608>
- [15] Collins, J. P. "Assessment and development of a tropospheric delay model for aircraft users of the global positioning system", Department of Geodesy and Geomatics Engineering Technical, University of New Brunswick, Fredericton, New Brunswick, Canada, Report No. 203, 1999.
- [16] Black, H. D., Eisner, A. "Correcting Satellite Doppler Data for Tropospheric Effects", *Journal of Geophysical Research*, 89(D2), pp. 2616–2626, 1984.  
<https://doi.org/10.1029/JD089iD02p02616>
- [17] Lagler, K., Schindelegger, M., Böhm, J., Krásná, H., Nilsson, T. "GPT2: Empirical slant delay model for radio space geodetic techniques", *Geophysical Research Letters*, 40(6), pp. 1069–1073, 2013.  
<https://doi.org/10.1002/grl.50288>
- [18] Dee, D. P., Uppala, S. M., Simmons, A. J., Berrisford, P., Poli, P., Kobayashi, S., Andrae, et al. "The ERA-Interim reanalysis: Configuration and performance of the data assimilation system", *Quarterly Journal of the Royal Meteorological Society*, 137(656), pp. 553–597, 2011.  
<https://doi.org/10.1002/qj.828>
- [19] Saastamoinen, J. "Contributions to the theory of atmospheric refraction", *Bulletin Géodésique*, 107(1), pp. 13–34, 1973.  
<https://doi.org/10.1007/BF02522083>
- [20] Inyurt, S., Yildirim, O., Mekik, C. "Comparison between IRI-2012 and GPS-TEC observations over the western Black Sea", *Annales Geophysicae*, 35(4), pp. 817–824, 2017.  
<https://doi.org/10.5194/angeo-35-817-2017>
- [21] Jan, S.-S. "Vertical guidance performance analysis of the L1-L5 dual-frequency GPS/WAAS user avionics sensor", *Sensors*, 10(4), pp. 2609–2625, 2010.  
<https://doi.org/10.3390/s100402609>
- [22] ICAO "ICAO Annex 10-Volume I Aeronautical Telecommunications - Radio Navigation Aids", Montréal, ICAO, Québec, Canada 2006.
- [23] Speidel, J., Tossaint, M., Wallner, S., Ávila-Rodríguez, J. A. "Integrity for Aviation: Comparing Future Concepts", *Inside GNSS*, pp. 54–64, 2013. Available at <http://insidegnss.com/wp-content/uploads/2018/01/julyaug13-WP.pdf> [Accessed: 04.12.2018]
- [24] ISO "ISO 2533:1975 Standard Atmosphere", International Organization for Standardization (ISO), Geneva, Switzerland, 1975.
- [25] Rocken, C., Sokolovskiy, S., Johnson, J. M., Hunt, D. "Improved mapping of tropospheric delays", *Journal of Atmospheric and Oceanic Technology*, 18(7), pp. 1205–1213, 2001.  
[https://doi.org/10.1175/1520-0426\(2001\)018<1205:IMOTD>2.0.CO;2](https://doi.org/10.1175/1520-0426(2001)018<1205:IMOTD>2.0.CO;2)
- [26] Essen, L., Froome, K. D. "The refractive indices and dielectric constants of air and its principal constituents at 24,000 Mc/s", *Proceedings of the Physical Society. Section B*, 64(10), pp. 862–875, 1951.  
<https://doi.org/10.1088/0370-1301/64/10/303>
- [27] Thayer, G. D. "An improved equation for the radio refractive index of air", *Radio Science*, 9(10), pp. 803–807, 1974.  
<https://doi.org/10.1029/RS009i010p00803>